

# Consistent and Invariant Generalization Learning for Short-video Misinformation Detection

Hanghui Guo  
Zhejiang Normal University  
Zhejiang, China  
ghh1125@zjnu.edu.cn

Weijie Shi  
HKUST  
Hong Kong SAR, China

Mengze Li  
HKUST  
Hong Kong SAR, China

Juncheng Li  
Zhejiang University  
Zhejiang, China

Hao Chen  
Tencent  
China

Yue Cui  
HKUST  
Hong Kong SAR, China

Jiajie Xu  
Soochow University  
Jiangsu, China

Jia Zhu  
Zhejiang Normal University  
Zhejiang, China

Jiawei Shen  
Zhejiang Normal University  
Zhejiang, China

Zhangze Chen  
Zhejiang Normal University  
Zhejiang, China

Sirui Han  
HKUST  
Hong Kong SAR, China

## ABSTRACT

Short-video misinformation detection has attracted wide attention in the multi-modal domain, aiming to accurately identify the misinformation in the video format accompanied by the corresponding audio. Despite significant advancements, current models in this field, trained on particular domains (source domains), often exhibit unsatisfactory performance on unseen domains (target domains) due to domain gaps. To effectively realize such *domain generalization* on the short-video misinformation detection task, we propose deep insights into the characteristics of different domains: (1) The detection on various domains may mainly rely on different modalities (*i.e.*, mainly focusing on videos or audios). To enhance domain generalization, it is crucial to achieve optimal model performance on all modalities simultaneously. (2) For some domains focusing on cross-modal joint fraud, a comprehensive analysis relying on cross-modal fusion is necessary. However, domain biases located in each modality (especially in each frame of videos) will be accumulated in this fusion process, which may seriously damage the final identification of misinformation. To address these issues, we propose a new Domain generalization model via Consistency and invariance learning for short-video misinformation detection (named **DOCTOR**), which contains two characteristic modules: (1) We involve the cross-modal feature interpolation to map multiple modalities into

a shared space and the interpolation distillation to synchronize multi-modal learning; (2) We design the diffusion model to add noise to retain core features of multi modal and enhance domain invariant features through cross-modal guided denoising. Extensive experiments demonstrate the effectiveness of our proposed DOCTOR model. Our code is publicly available at <https://github.com/ghh1125/DOCTOR>.

## CCS CONCEPTS

• Information systems → Multimedia information systems; • Computing methodologies → Transfer learning.

## KEYWORDS

Misinformation Detection; Domain Generalization; Multi-modal

### ACM Reference Format:

Hanghui Guo, Weijie Shi, Mengze Li, Juncheng Li, Hao Chen, Yue Cui, Jiajie Xu, Jia Zhu, Jiawei Shen, Zhangze Chen, and Sirui Han. 2025. Consistent and Invariant Generalization Learning for Short-video Misinformation Detection. In *Proceedings of Make sure to enter the correct conference title from your rights confirmation email (ACM Multimedia 2025)*. ACM, New York, NY, USA, 15 pages. <https://doi.org/XXXXXXXX.XXXXXXX>

## 1 INTRODUCTION

With the rapid rise of short video platforms like TikTok, misinformation in the short-video format accompanied by matching audio is spreading rapidly and widely [2, 6, 48, 52]. Such short-video misinformation may seriously mislead public decision-making and behavior, which poses a potential threat to social stability [3, 39].

Hence, there is an urgent requirement to develop effective methods for promptly identifying misinformation to control its spread [26]. Benefiting from the development of deep learning technology, existing methods achieve promising results in this field [6, 47]. Nevertheless, when trained on specific domains (source domains  $\mathcal{D}_s$ ), these data-driven methodologies experience a notable decline in performance when directly being applied to unseen domains (target domains  $\mathcal{D}_t$ ) [37]. The failure of such *domain generalization* is

Hanghui Guo and Jia Zhu are with the Zhejiang Key Laboratory of Intelligent Education Technology and Application, Zhejiang Normal University.

Permission to make digital or hard copies of all or part of this work for personal or classroom use is granted without fee provided that copies are not made or distributed for profit or commercial advantage and that copies bear this notice and the full citation on the first page. Copyrights for components of this work owned by others than the author(s) must be honored. Abstracting with credit is permitted. To copy otherwise, or republish, to post on servers or to redistribute to lists, requires prior specific permission and/or a fee. Request permissions from [permissions@acm.org](mailto:permissions@acm.org).

ACM Multimedia 2025, October 27–31, 2025, Dublin, Ireland

© 2025 Copyright held by the owner/author(s). Publication rights licensed to ACM.

ACM ISBN 978-x-xxxx-xxxx-x/YY/MM...\$15.00

<https://doi.org/XXXXXXXX.XXXXXXX>

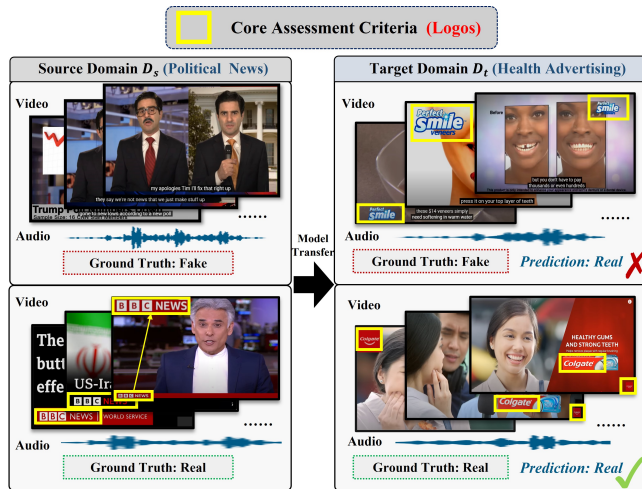


Figure 1: An example of how *domain bias* (like logos) can lead to errors in misinformation detecting of the target domain.

primarily attributed to the existence of substantial differences in data distribution across various domains. Figure 1 illustrates an example where, in the political news domains, many logos mean information coming from official media, which may represent its authenticity; whereas, in health advertising domains, almost all short videos (*i.e.*, real and fake ones) are accompanied by product logos. This shift of *domain bias* leads to detection errors of misinformation.

To effectively realize the domain generalization on the short-video misinformation detection task, we provide deep insights into the characteristics of different domains. In particular, various domains exhibit distinct forms of fraud, encompassing activities such as news falsification focused on a single modality as well as the convergence of multiple modalities for deceptive purposes. Due to the existing domain gap, designing methods to generalize to diverse domains will encounter different problems:

**(1) Varying Modal-dependence in Different Domains.** In cases where particular modal information in short-video news is falsified (like only falsifying video or audio), various domains may prioritize different types of modalities for their focus [6, 17, 20]. To fully enhance the domain generalization, the reasoning ability in any modality should be fully optimized when training misinformation detection models [29, 46]. However, during such cross-modal joint learning, multiple modalities may compete with each other. This may ultimately lead to insufficient knowledge acquisition for parts of modalities, making it challenging to achieve the sweet point on all modalities simultaneously.

**(2) Domain-bias Enhancement in Cross-modal Fusion.** For news falsification on multiple modalities together, a comprehensive analysis based on effective cross-modal fusion is necessary for accurate falsification detection [16, 19, 42]. However, as detailed shown in Figure 2, simply summing the features of all modalities will add up the domain bias located in the features of each modality. In particular, video features introduced may be accompanied by a significant accumulation of domain bias stemming from the numerous non-core video frames and the non-core frame areas involved. Such bias accumulation from all modalities seriously highlights bias impact in the obtained feature and damages the final detection.

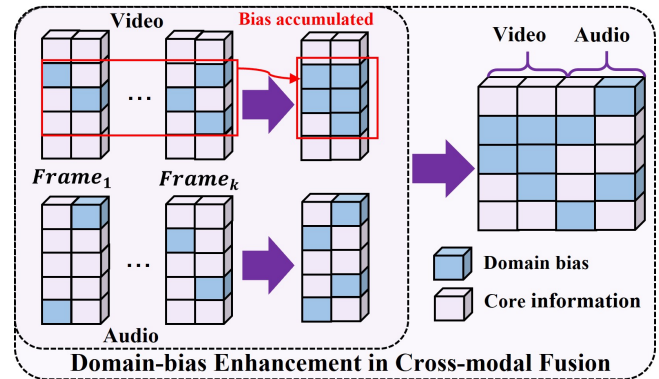


Figure 2: The problem of *Domain-bias Enhancement in Cross-modal Fusion*. The red line is a simple case of *bias accumulated* (Audio bias and fusion bias accumulated are consistent with the video, so we have omitted them in this figure).

To tackle the aforementioned issues, we introduce a new DOmain generalization model via Consistency and invariance learning for shORT-video misinformation detection (named **DOCTOR**). Specifically, there are two specific designs: **(1) Cross-modal Interpolation Distillation.** We project video and audio modality features into a shared representation space, and mix these representations with a random mixing ratio to construct interpolations. Based on the feature distribution of these interpolation samples as teacher signals, feature distillation drives the learning optimization process of the student model, making the representation learning across modalities more consistent and synchronized. **(2) Multi-modal Invariance Fusion.** Incorporating subtitles extracted from each video frame as a guide, we devise a novel mechanism to facilitate the extraction of core video features from both spatial and temporal viewpoints. With extracted multi-modal features, we add noise to them step by step based on the diffusion model to filter out redundant details, thereby underlining the core features of multi-modal. Subsequently, by gradually mitigating the noise influence, we further outline the fundamental information of multi-modal features through cross-modal mutual guidance, boosting domain invariant features.

The main contributions of our work are as follows:

- To the best of our knowledge, we take the early exploration of the domain generalization on the short-video misinformation detection task. For this new setting, we introduce the DOCTOR model via consistency and invariance learning.
- We propose distillation for the cross-modal feature interpolation to coordinate model learning of multiple modalities. In addition, we involve diffusion-based domain bias filtering and invariant feature learning by step-by-step adding noise and denoising.
- We validate the effectiveness of our DOCTOR model through extensive comparative experiments.

## 2 RELATED WORKS

### 2.1 Multi-modal Misinformation Detection

Early research on multi-modal misinformation detection primarily focuses on text and image, emphasizing cross-modal correlation [21, 22, 35, 45, 48, 49]. For example, MCAN [38] designs co-attention networks to fuse textual and visual features. CAFE

[8] transforms features into a shared semantic space through cross-modal semantic alignment and combines cross-modal fuzzy learning to estimate the fuzziness between different modalities. MMICF [44] introduces the causal inference module to eliminate the direct disparity in the fusion between text and image entities through causalities. Although these methods have shown promising performance in detecting misinformation involving text and images, their direct applicability to short-video misinformation is limited due to fundamental differences in content production mechanisms [5].

With the rise of online short-video platforms, the spread of misinformation has expanded to video-audio. Some short-video misinformation detection methods have been proposed through recent research for these situations. OpEvFake [52] employs a large language model to mine implicit viewpoints in short videos and combines model information to enhance interaction for judgment. SV-FEND [28] exploits cross-modal correlations to select the most informative features and uses social context information for detection. FakingRecipe [6] detects misinformation by simulating the creation process of audio and video. TikTec [31] employs speech text-guided visual object features and MFCC-guided speech textual features. However, these methods are typically designed for general domains and often underperform in domain generalization scenarios.

## 2.2 Multi-modal Domain Generalization

While uni-modal domain generalization has been well-studied (such as only text, image, or video), research on video-audio domain generalization remains limited [24, 25, 40]. Some of the recent progress on video-audio includes: SimMMDG [11] improves domain generalization by increasing the distance between modality-specific features and modality-shared features of audio and video. CMRF [13] improves domain generalization by reducing the flat minima between different modalities. RNA-Net [27] balances audio and video feature norms via a relative norm alignment loss to enhance domain generalization. However, the existing domain generalization focus on video-audio methods is primarily tailored for general domains rather than specifically designed for misinformation detection, resulting in limited task adaptability and suboptimal performance.

In contrast, domain generalization for misinformation has currently focused on text-image modalities, using domain-aware fusion and representation learning [7, 32, 33, 50]. For instance, EDDFN [32] learns features from domain-specific and cross-domain embeddings and then connects domain-related knowledge. MDFEND [23] aggregates multiple representations extracted by experts through domain gates. MDMFND [33] integrates cross-domain and domain-specific knowledge through the design of expert networks and step-by-step pivot transformers. However, these methods rely on static alignment, which is inadequate for video-audio data that involve temporal dynamics and complex interactions [36, 51]. Therefore, bridging the domain generalization gap in short-video misinformation detection remains an urgent and underexplored challenge.

## 3 PROPOSED METHOD: DOCTOR

In this section, we propose an innovative DOmain generalization model via Consistency and invariance learning for shORT-video misinformation detection (named **DOCTOR**). We will present each module and its training strategy in detail as follows.

### 3.1 Model Overview

**3.1.1 Problem Formulation. Short-video misinformation detection.** We assume that the input is a short video  $v$  and accompanying audio  $a$  (sometimes matched with a text description  $t$  about the video title or introduction). After judging whether it contains misinformation, the output predicted label is represented as  $Y \in \{0, 1\}$ , where 0 represents misinformation and 1 represents the opposite. Building a misinformation detection model  $\mathcal{M}$ , input multi-modal data  $\{v, a, t\}$ , output predicted labels  $\hat{Y}$ , we minimize the loss function  $\mathcal{L}(\cdot)$  between the predicted label  $\hat{Y}$  and the true label  $Y$  by optimizing the parameter  $\Theta$ . The following is the target formula:

$$\min_{\Theta} \mathbb{E}_{(v,a,t,Y) \sim D} [\mathcal{L}(Y, \hat{Y})], \quad \hat{Y} = \mathcal{M}(v, a, t; \Theta), \quad (1)$$

where  $D$  is the joint distribution over all inputs and labels.

**Domain generalization for short-video misinformation detection.** In practical applications, short-video misinformation detection models trained on source domains may need to infer on unseen target domains, and the data distribution of these target domains may be different from source domains. We aim to propose specific modules to enhance the robust feature learning on the source domains  $\mathcal{D}_s$  to further improve the model performance on the target domains  $\mathcal{D}_t$ .

**3.1.2 Overview of DOCTOR.** As illustrated in Figure 3, which demonstrates the domain generalization for the short-video misinformation detection task, the proposed model, **DOCTOR**, is designed to address the generalization gap between source and target domains.

The training process of the DOCTOR model is carried out in an end-to-end manner, consisting of two key modules that synchronize for optimization, jointly improving the model’s domain generalization ability: (1) Cross-modal Interpolation Distillation: Construct interpolation features for video and audio modalities during the training process, and use them as teacher signals to guide student models to learn consistent and aligned representations between modalities. (2) Cross-modal Invariance Fusion: Construct multi-modal features and optimize them through a diffusion denoising mechanism, gradually enhancing the cross-domain invariance and discriminative power of the multi-modal representations.

The two modules are synchronously executed during the training process, jointly driving the model to learn robust representations from the perspectives of consistency and invariance, thereby improving generalization performance in the target domain.

### 3.2 Cross-modal Interpolation Distillation

In many domains, information falsification tends to be focused on distinct modalities (i.e., solely focusing on video or audio falsification). Enhancing domain generalization on them requires us to comprehensively integrate the inferential capabilities of each modality. However, in the cross-modal joint learning processes, multiple modalities may compete with each other, which can ultimately lead to insufficient knowledge acquisition in particular modalities and thus prevent optimal performance. To address this issue, we propose **Cross-modal Interpolation Distillation**.

Following the existing misinformation detection work [6], we utilize fine-tuned versions of HuBERT [15] as an encoder to extract audio features  $X_a$ , and Vision Transformer (ViT) [12] as an encoder to extract video features  $X_v$ .

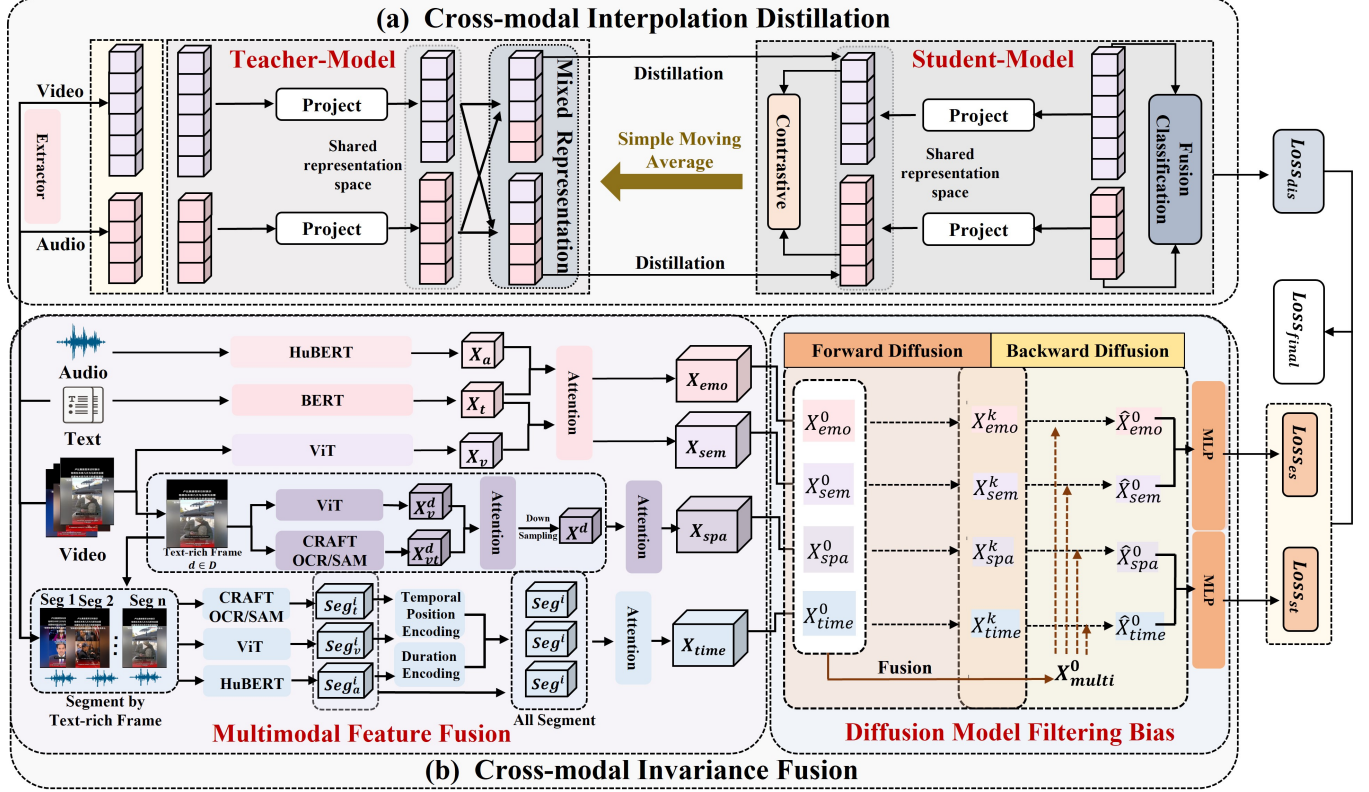


**Figure 3: The architecture of the DOCTOR model. (a) Cross-modal Interpolation Distillation: Video and audio modality features are projected into a shared representation space and mixed with a random ratio to create interpolation samples. These samples are then used as teacher signals to guide the student model in learning consistent representations across modalities. (b) Cross-modal Invariance Fusion: Multi-modal features are first fused, and then progressively perturbed through a diffusion model to mask domain biases. The noise is gradually removed to enhance the core features of multi-modal, with the goal of obtaining domain-invariant features.**

Due to the heterogeneity of modalities, the dimensions of the extracted features vary. Therefore, we employ the **Project** method to map the features of the video and audio modalities into a shared representation space, where all modalities have a unified dimension of  $d$ . In this shared representation space, we can directly establish connections between the different modalities. The unified dimensional feature representation we obtain is:  $\hat{X}_k, k \in a, v$ .

$$\hat{X}_k = P_k(X_k) \in \mathcal{R}^d, \quad (2)$$

where  $P_k$  is the Project (different modal  $k$  using different Project) and  $k$  represents different modalities ( $a$ : Audio,  $v$ : Video).

Then, in order to enhance the knowledge utilization of each modality in the cross-modal joint learning process and make the cross-modal representation more consistent in the shared representation space, we construct the interpolation representation between them through cross-modal representation mixup  $\hat{X}_{a,v}$ :

$$\hat{X}_{a,v} = \theta \hat{X}_a + (1 - \theta) \hat{X}_v, \quad (3)$$

where  $\theta$  is a mixing ratio.

If the loss of mixed representation  $\hat{X}_{a,v}$  can be optimized to lower values, we can achieve the best state in all modalities at the same time. However, the amount of computation in multi-modal learning is often huge, and it is often difficult to achieve the optimal state, which

is impractical in practical applications. Thus, we adopt the cross-modal distillation technique to distill the knowledge in the mixed representation into each modality and then optimize the learned representation to achieve the best state in all modalities. Specifically, as follows, for each modal  $k \in (a$ : Audio,  $v$ : Video), we initialize the student model  $\gamma_t^k$  and utilize Simple Moving Average (SMA) to create the teacher model  $\hat{\gamma}_t^k$ , which is used to generate more stable and generalizable representations. The  $\hat{\gamma}_t^k$  represents as:

$$\hat{\gamma}_t^k = \begin{cases} \gamma_t^k, & \text{if } t \leq t_0 \\ \frac{t-t_0}{t-t_0+1} \cdot \hat{\gamma}_{t-1}^k + \frac{1}{t-t_0+1} \cdot \gamma_t^k, & \text{if } t > t_0 \end{cases} \quad (4)$$

where  $\gamma_t^k$  means that iteration  $t$  is the student mode state of modal  $k$ , and  $t_0$  is the number of iterations at which to start the SMA. Therefore, the representation produced by the teacher model  $\hat{\gamma}_t^k$  is denoted as  $\hat{X}_k$ , which serves as a stable reference for the modality  $k$ . Based on this, we obtain a new cross-modal representation mixup  $\hat{X}_{a,v}$  as follows:

$$\hat{X}_{a,v} = \theta \hat{X}_a + (1 - \theta) \hat{X}_v. \quad (5)$$

In the process of knowledge distillation and hybrid representation generation, in order to provide a flexible and controllable interpolation method when generating hybrid samples  $\hat{X}_{a,v}$ , we adopt Beta

distribution. We define  $\theta$  as ( $\theta \sim \text{Beta}(\alpha, \alpha)$ ) and  $\alpha$  is a hyperparameter in the Beta distribution.

Due to the semantic gap between the modalities, we introduce a dynamic threshold  $\theta$  to distinguish the dominance of different modalities and use the interpolated features of the modality closer to the  $k$  modality ( $k \in (a : \text{Audio}, v : \text{Video})$ ) as the teacher signal to achieve cross-modal knowledge transfer. Therefore, the distillation loss should be specifically as follows:

$$\begin{aligned} L_{\text{dis}}^v &= \|\hat{X}_v - \hat{X}_{v,a}\|_2^2, & \theta \leq 0.5 \\ L_{\text{dis}}^a &= \|\hat{X}_a - \hat{X}_{v,a}\|_2^2, & \theta > 0.5 \end{aligned} \quad (6)$$

Afterward, we assign a dedicated classifier to each modality before the *Project* in the student model and optimize the features by the classification loss  $L_{cls}^a$  and  $L_{cls}^v$ .

In addition, to bridge the gap between audio and video modalities and make the representations of each modality more consistent and synchronized, we further employ multi-modal supervised contrastive learning on a shared representation space. The contrastive learning loss formula is as follows:

$$L_{con} = -\frac{1}{|B|} \sum_{i \in B} \log \frac{\exp(\hat{X}_a^i \cdot \hat{X}_v^i / \tau)}{\sum_{\substack{j \in B \\ j \neq i}} \left[ \exp(\hat{X}_a^i \cdot \hat{X}_a^j / \tau) + \exp(\hat{X}_a^i \cdot \hat{X}_v^j / \tau) \right]}, \quad (7)$$

where  $B$  is the sample set in the training batch,  $\tau$  is the temperature coefficient,  $\exp(\cdot/\tau)$  is a similarity scaling function used to adjust the discrimination between positive and negative samples, and  $\hat{X}_a^i, \hat{X}_v^i$  are the audio and video modality embedding vectors of sample  $i$ .

Finally, we combine the losses of the above steps to obtain the final Cross-modal Interpolation Distillation loss:  $Loss_{dis}$ .

$$Loss_{dis} = L_{con} + L_{cls}^a + L_{cls}^v + L_{dis}^a + L_{dis}^v. \quad (8)$$

### 3.3 Cross-modal Invariance Fusion

When multi-modal joint fraud is emphasized in many domains, the separate process of each modality may not be adequate to enhance model generalization across these domains. Therefore, we need to comprehensively analyze cross-modal fusion features. However, direct fusion cross-modal features will accumulate the domain bias of each modality. In particular, for the video modality, domain biases present in numerous non-core video frames and non-core frame areas involved may accumulate significantly through the fusion of frames and areas on a frame-by-frame and area-by-area basis.

Toward this issue, we propose an innovative method: **Cross-modal Invariance Fusion**. It designs a novel mechanism for performing core extraction for video features from spatial and temporal perspectives. With extracted multi-modal features, we add noise to them step by step based on the diffusion model to filter out redundant details, thereby underlining the core features of multi-modal. Subsequently, by gradually mitigating the noise influence, we further outline the core information of multi-modal features through cross-modal mutual guidance, enhancing domain invariant features. We aim to mitigate the impact of domain bias and retain domain invariance to enhance the domain generalization ability for misinformation detection. In detail, it includes the following two steps:

**3.3.1 Multimodal Feature Fusion.** For domain invariance of the *spatial features* in the video, we consider that creators of misinformation often add misleading elements, such as subtitles, to disguise forged frames. Thus, we select text-rich frames ( $F_d, d \in D$ , where  $D$  represents the set of all text-rich frames) as starting points. The extraction process for spatial features is detailed in Algorithm 1 (**for the detailed steps, see Supplementary Material A**). Following the steps below, we obtain the spatial features  $X_{spa}$ .

---

#### Algorithm 1 Spatial Feature Extraction

---

**Require:** Frame  $F_d$ , Text Area ( $TA$ )

**Ensure:** Spatial feature representation  $X_{spa}$

- 1: **Text Area Detection and Embedding:**
  - 2: Apply CRAFT OCR to detect  $TA$  in frame  $F_d$
  - 3: Convert  $TA$  to prompt embeddings  $X_{ot}^d$  using SAM (Segment Anything Model) prompt encode
  - 4: **Initial Visual Encoding:**
  - 5: Input  $F_d$  into pre-trained ViT to generate initial encoding  $X_v^d$
  - 6: **Bidirectional Attention Block:**
  - 7: *Self-Attention for Text Features:*
  - 8:  $\hat{X}_{ot}^d = \text{NORM}(X_{ot}^d + \text{Self-Att}(X_{ot}^d))$
  - 9: *Cross-Attention between Text and Visual Features:*
  - 10:  $\hat{X}_{ot}^d = \text{NORM}(\hat{X}_{ot}^d + \text{Cross-Att}(\hat{X}_{ot}^d, X_v^d))$
  - 11: *Cross-Attention for Enhanced Visual Features:*
  - 12:  $\hat{X}_v^d = \text{NORM}(X_v^d + \text{Cross-Att}(\text{MLP}(\hat{X}_{ot}^d), X_v^d))$
  - 13: **Spatial Feature Extraction:**
  - 14: Downsample  $\hat{X}_v^d$  through two convolutional layers
  - 15: Expand to obtain single-frame spatial pattern features  $X^d$
  - 16: **Multi-Frame Feature Fusion:**
  - 17: Fuse all frame features:  $\text{Self-Att}([X^1, X^2, \dots, X^d])$
  - 18: Average pooling:  $X_{spa} = \text{MEAN}(\text{Self-Att}([X^1, X^2, \dots, X^d]))$
  - 19: **return**  $X_{spa}$
- 

To capture *temporal features* in multi-modal content, we segment videos using text-rich frames  $F_d$  as semantic anchors, as they typically encapsulate preceding context and exploit cognitive biases in visual memory—crucial for surfacing latent misinformation.

We represent each modality as a sequence of segments:  $\text{Text} = (T_1, I_1), (T_2, I_2) \dots (T_n, I_n)$ ,  $\text{Video} = (V_1, I_1), \dots (V_n, I_n)$ ,  $\text{Audio} = (A_1, I_1), \dots (A_n, I_n)$ , where  $T_k$  denotes the  $k$ -th text segment (subtitle),  $V_k$  and  $A_k$  are the corresponding video frame and audio clip at interval  $I_k$ . The rate (fps) and total frames (vframes) are included to represent duration. We first model the temporal structure of each modality independently, followed by a cross-modal interaction phase to capture joint temporal editing patterns. For each time-aligned segment, we extract modality-specific features: text subtitles are encoded using BERT [10] to obtain  $\text{Seg}_t^i$ , while video and audio features ( $\text{Seg}_v^i, \text{Seg}_a^i$ ) are fused via self-attention.

To further capture temporal dynamics, we introduce two encoding strategies: Temporal Position Encoding (TPE) and Duration Encoding (DE). TPE uses equal-frequency binning to assign learnable embeddings based on both absolute and relative segment durations. DE employs sinusoidal functions to represent segment positions within the video. These obtain  $TPE^i$  and  $DE^i$  of the segment  $i$ .

The final segment representation is constructed as:

$$\text{Seg}^i = DE^i + TPE^i + \text{Seg}_t^i + \text{Seg}_v^i + \text{Seg}_a^i. \quad (9)$$

Lastly, all segments are then fused via self-attention (Self-Att) to obtain the overall temporal representation  $X_{time}$ :

$$X_{time} = \text{MEAN}(\text{Self-Att}([Seg^1, Seg^2, \dots, Seg^i])). \quad (10)$$

**3.3.2 Diffusion Model Filtering Bias.** After obtaining the temporal feature  $X_{time}$  and the spatial feature  $X_{spa}$ , we feed them into a diffusion model that progressively injects noise to filter out domain biases and highlight multi-modal features' core information; as the noise influence gradually diminishes, we leverage cross-modal interactions to further accentuate the fundamental information of misinformation forgery, boosting domain invariant features.

To more effectively capture the domain invariant features, we incorporate semantic and emotional features during the diffusion process, as they provide intent interpretability and contextual awareness for spatiotemporal features. Based on the analysis of previous studies [6], different modalities play a dominant role in conveying information: audio mainly expresses emotions, text (News Introduction and Title) conveys semantic information while also presenting emotional colors, and video usually supplements text to convey semantic content. We utilize the BERT to encode text, HuBERT to encode audio, and ViT to encode video to separately get  $X_t$ ,  $X_a$ ,  $X_v$ . The attention mechanism is used to obtain the emotional features  $X_{emo}$  via  $X_t$  and  $X_a$ , and the semantic features  $X_{sem}$  via  $X_t$  and  $X_v$ .

Based on the above multi-modal features, the diffusion model we designed has the following steps:

**In the forward diffusion process**, we denote the initial distribution of each fusion feature as  $X_{emo}^0$  (emotion feature),  $X_{sem}^0$  (semantic feature),  $X_{spa}^0$  (spatial feature),  $X_{time}^0$  (temporal feature). For each feature, we gradually incorporate noise sampled from a Gaussian distribution into the true distribution. The steps are as follows:

$$q(X_F^k | X_F^{k-1}) = \mathcal{N}(X_F^{k-1}; X_F^k \sqrt{1 - \beta_F^k}, I \beta_F^k), \quad (11)$$

where the equation follows the Markov chain principle and represents the distribution of  $X_F^k$  under  $X_F^{k-1}$ ,  $\beta_F^k$  is a weight and indicates the proportion of noise added at the  $k$ -th step.  $I$  represents the identity matrix, which is used to control the covariance structure of the noise.  $F$  is a different feature of emo feature, sem feature, spa feature, and time feature.  $X_F^k$  can be sampled through the following process:

$$X_F^k = x_F^0 \sqrt{\prod_{i=1}^k \alpha_F^i} + \epsilon \sqrt{1 - \prod_{i=1}^k \alpha_F^i}, \quad \alpha_F^i = 1 - \beta_F^i, \quad (12)$$

where  $\epsilon$  is the noise sampled from  $\mathcal{N}(0, I)$ . The overall noise injection process is as follows, effectively filtering out redundant biases:

$$q(X_F^{1:K} | X_F^0) = \prod_{k=1}^K q(X_F^k | X_F^{k-1}). \quad (13)$$

**In the backward diffusion process**, we further enhance each basic feature by gradually alleviating the effect of noise and leveraging cross-modal features to guide each other. Specifically, we first fuse  $X_{emo}^0$ ,  $X_{sem}^0$ ,  $X_{spa}^0$ ,  $X_{time}^0$  into a mixed multi-features representation  $X_{multi}^0$  through a full connect layer denoted by  $\mathcal{F}_{fc}$ .

$$X_{multi}^0 = \mathcal{F}_{fc}(X_{emo}^0 \oplus X_{sem}^0 \oplus X_{spa}^0 \oplus X_{time}^0). \quad (14)$$

Then, the noise injection feature representation  $X_{emo}^k, X_{sem}^k, X_{spa}^k, X_{time}^k$  obtained in the first step is combined with the fused multi-features representation  $X_{multi}^0$  to gradually predict the distribution of each feature representation in the denoising model. In this way, each multi-modal feature, based on the information of other features, guides each other to restore the core features (the invariance characteristics of different domains misinformation forgery) of each modality to the greatest extent, so as to reduce the interference of domain bias. The specific steps are as follows:

$$p(X_F^{k-1} | X_F^k) = \mathcal{N}(X_F^{k-1}; \mu_\theta(X_F^k, X_{multi}^0, k), \Sigma_\theta(k)), \quad (15)$$

where  $\mu_\theta$  is the predicted mean (indicating the direction of denoising), and  $\Sigma_\theta(k)$  is the covariance of the noise. This process gradually generates  $X_F^{k-1}, X_F^{k-2}, \dots, X_F^0$  from  $X_F^k$  that is, gradual denoising.

In total, under the optimization of the multi-feature cross-modal guided diffusion model, we can minimize the domain bias of misinformation domain generalization to retain the invariant of misinformation in different domains in the features.

Finally, we separately input the optimization features  $\hat{X}_{emo}^0$  and  $\hat{X}_{sem}^0, \hat{X}_{spa}^0$  and  $\hat{X}_{time}^0$  into the MLP for prediction.

## 4 EXPERIMENTS

### 4.1 Experimental Setups

**4.1.1 Datasets.** (1) **FakeSV** [28]: This dataset is the largest public Chinese video, audio, and text misinformation detection dataset, containing samples from two popular Chinese short-video platforms, TikTok and Kuaishou, covering news in multiple domains. (2) **FakeTT** [6]: This dataset is a public English video, audio, and text misinformation detection dataset that focuses on videos related to events reported by the fact-checking website Snopes.

We use the Qwen2.5-72B [41] combined with manual verification for label classification. We divide into nine domains (Society, Health, Disaster, Culture, Education, Finance, Politics, Science, and Military). See Supplementary Material B for the detailed steps.

**4.1.2 Baselines.** We selected some popular misinformation short-video detection methods, such as FakingRecipe [6], OpEvFake [52], TikTec [31], HCFC-Hou [14], HCFC-Medina [30], FANVM [9], SV-FEND [28]. We also compared with the novel **general domain generalization** method CMRF [13] and the **text-image misinformation domain generalization** methods MDMFND [33] and DMFEND [23]. We also select GPT-4 [1] and GPT-4V [43] for comparison.

**4.1.3 Implementations.** All of our experiments were conducted on an NVIDIA RTX A6000. We set the learning rate as 5e-5 for FakeSV and 1e-3 for FakeTT. Specifically, for more information, see Supplementary Material C.

### 4.2 Experimental Results

**4.2.1 Domain generalization experiments.** To evaluate DOCTOR in domain generalization, we show in Table 1 that DOCTOR consistently outperforms other methods across all domains.

Specifically, compared with the recent state-of-the-art method for general domain generalization in video and audio, CMRF, our proposed DOCTOR model demonstrates a superior ability to effectively leverage multi-modal information while mitigating domain bias,

**Table 1: Performance comparison of domain generalization accuracy of different methods with DOCTOR on FakeSV and FakeTT datasets, and perform an ablation study on two key components (Section 3.2: Distillation and Section 3.3: Diffusion) of DOCTOR in domain generalization. \* represents the domain generalization method.**

Dataset	Method	Disaster	Society	Health	Culture	Politics	Science	Education	Finance	Military
FakeSV	FakingRecipe	78.79	75.85	81.44	85.16	65.08	85.27	73.26	73.11	87.30
	SV-FEND	76.36	73.96	80.13	82.69	65.11	82.76	70.45	72.67	86.96
	OpEvFake	79.54	74.76	81.43	85.34	75.74	87.05	77.54	80.12	90.57
	CMRF*	79.76	74.45	81.28	84.77	74.49	86.56	76.32	80.76	91.87
	MDFEND*	61.39	51.13	69.87	78.36	55.28	79.74	71.33	59.26	66.65
	M MDFEND*	75.49	73.10	78.97	82.57	72.58	82.75	74.28	79.13	86.67
	<b>DOCTOR</b>	<b>81.67</b>	<b>77.15</b>	<b>83.66</b>	<b>86.26</b>	<b>77.16</b>	<b>88.34</b>	<b>78.22</b>	<b>83.87</b>	<b>93.65</b>
	w/o Diffusion	79.82	76.05	82.46	85.81	76.58	87.73	77.22	82.67	92.36
	w/o Distillation	80.57	75.97	81.75	85.71	75.86	87.11	77.34	81.72	91.45
Dataset	Method	Disaster	Society	Health	Culture	Politics	Science	{Education, Finance, Military}		
FakeTT	FakingRecipe	71.37	71.21	76.03	79.62	55.66	76.75	77.78		
	SV-FEND	70.21	70.85	76.53	77.79	57.34	75.15	72.89		
	OpEvFake	71.84	76.67	84.21	83.56	66.89	77.50	79.98		
	CMRF*	71.75	77.05	81.87	83.47	65.78	74.96	81.43		
	MDFEND*	62.23	66.58	52.73	78.96	59.66	70.13	52.93		
	M MDFEND*	70.08	75.57	76.89	82.46	63.44	74.90	71.85		
	<b>DOCTOR</b>	<b>74.18</b>	<b>78.34</b>	<b>85.33</b>	<b>88.31</b>	<b>70.33</b>	<b>78.23</b>	<b>86.11</b>		
	w/o Diffusion	73.52	77.97	84.47	85.18	67.83	76.38	85.18		
	w/o Distillation	72.45	77.44	83.77	84.61	68.95	77.85	81.72		

**Table 2: Comparison of general domain misinformation detection performance of different methods on FakeSV and FakeTT datasets.**

Dataset	Method	Acc.	F1	Fake Class			Real Class		
				Precision	Recall	F1	Precision	Recall	F1
FakeSV	FakingRecipe	82.83	82.62	85.28	83.88	84.58	79.84	81.51	80.67
	GPT-4	67.43	67.34	83.71	53.99	65.64	57.81	85.71	69.05
	GPT-4V	69.15	69.14	82.35	58.78	68.60	60.00	83.08	69.68
	FANVM	78.52	78.81	78.64	87.17	82.68	80.95	69.75	74.94
	SV-FEND	80.88	80.54	85.82	77.63	81.52	74.53	83.61	78.81
	TikTec	73.41	73.26	78.37	72.70	75.43	68.08	74.37	71.08
	HCFC-Medina	76.38	75.83	77.50	81.58	79.49	74.77	69.75	72.17
	HCFC-Hou	74.91	73.61	73.46	86.51	79.46	77.72	60.08	67.77
	<b>DOCTOR</b>	<b>84.91</b>	<b>84.70</b>	<b>84.80</b>	<b>91.57</b>	<b>86.67</b>	<b>83.46</b>	<b>82.57</b>	<b>83.67</b>
FakeTT	FakingRecipe	78.58	76.62	65.49	74.75	69.81	86.56	80.50	83.42
	GPT-4	61.45	60.66	43.36	75.61	55.11	83.19	55.00	66.22
	GPT-4V	58.69	58.69	44.52	88.46	59.23	88.00	43.42	58.15
	FANVM	71.57	70.21	55.15	75.76	63.83	85.28	69.50	76.58
	SV-FEND	77.14	75.63	62.33	78.79	69.57	87.91	76.33	81.69
	TikTec	66.22	65.08	49.32	72.73	58.78	82.35	63.00	71.39
	HCFC-Medina	62.54	62.23	46.24	80.81	58.82	84.92	53.50	65.64
	HCFC-Hou	73.24	72.00	56.93	78.79	66.10	87.04	70.50	77.90
	<b>DOCTOR</b>	<b>78.92</b>	<b>78.04</b>	<b>64.71</b>	<b>76.75</b>	<b>72.21</b>	<b>90.19</b>	<b>78.00</b>	<b>81.89</b>

thereby enhancing domain generalization in misinformation detection. As there is currently a lack of domain generalization methods

tailored for short-video misinformation detection, we additionally compare the DOCTOR model with M MDFEND and MDFEND,

which are SOTA methods (Open Source) for domain generalization in text-image misinformation detection. Across various domains, DOCTOR consistently achieves significantly higher accuracy.

Also, we compare with the recent SOTA short-video misinformation detection methods (such as FakingRecipe, SV-FEND, and OpEvFake). DOCTOR surpasses other models in terms of accuracy in domain generalization tests in the FakeSV and FakeTT datasets, reaching an average of 3% ~4% and effectively demonstrating the domain generalization ability of the DOCTOR model.

Finally, we conducted an ablation study on two key components of DOCTOR, Diffusion and Distillation, and found that the accuracy rate decreased. This indicates that these two components have an indispensable and effective synergy in the overall DOCTOR. They work together to provide key support for domain generalization.

Overall, DOCTOR outperforms other state-of-the-art methods in domain generalization for the following reasons: 1) DOCTOR designs interpolation knowledge distillation to solve the problem of modal competition caused by the need to make full use of multi-modal information when misinformation in different fields tends to be forged in different modalities. 2) DOCTOR is designed to diffuse comprehensive modal information, which effectively solves the problem of domain biases between different domains during domain collaboration. These designs fully improve the domain generalization ability of short-video misinformation detection.

**4.2.2 General domain experiments.** Another point worth discussing is whether solving the differences between different domains will interfere with misinformation detection in the general domain. As shown in Table 2, we conducted a thorough comparison using multiple indicators and multiple methods on two short-video misinformation detection datasets, FakeTT and FakeSV.

In the FakeSV dataset, DOCTOR achieved 84.91% accuracy and 84.70% F1. The overall performance is better than most existing short-video misinformation detection methods and some large language models. From the perspective of truth and misinformation, the DOCTOR is more effective in improving the method of identifying truth (Precision: 83.46%, Recall: 82.57%, F1: 83.67%). DOCTOR is also very competitive in identifying misinformation methods.

In the FakeTT dataset, DOCTOR also has great advantages, achieving 78.92% of accuracy and 78.04% of F1. This result surpasses other methods. Similarly, as mentioned above, there are similar performance trends in the real class and fake class.

**Table 3: Ablation Study Results of DOCTOR model on FakeSV and FakeTT Datasets in the general domain.**

Dataset	Method	F1	Acc.	AUC	Recall	Precision
FakeSV	<b>DOCTOR</b>	<b>84.70</b>	<b>84.91</b>	<b>83.82</b>	<b>83.82</b>	<b>84.62</b>
	w/o Diffusion	82.54	82.84	82.46	82.46	82.62
	w/o SE	83.76	83.67	82.76	82.76	82.98
	w/o ST	82.97	83.42	82.34	82.34	82.67
	w/o Distillation	82.90	83.21	82.79	82.79	83.03
FakeTT	<b>DOCTOR</b>	<b>78.04</b>	<b>78.92</b>	<b>77.37</b>	<b>77.37</b>	<b>76.44</b>
	w/o Diffusion	74.79	76.25	76.89	76.89	74.32
	w/o SE	76.63	77.54	76.87	76.87	74.54
	w/o ST	74.82	74.23	75.47	75.47	72.67
	w/o Distillation	76.44	77.92	76.87	76.87	75.85

**Table 4: Learning rate sensitivity results for DOCTOR model on FakeSV and FakeTT datasets (Accuracy).**

Dataset	1e-5	5e-5	1e-4	5e-4	1e-3	5e-3
FakeSV	82.32	84.91	83.45	80.78	79.53	78.44
FakeTT	72.24	74.31	76.86	78.57	78.92	77.39

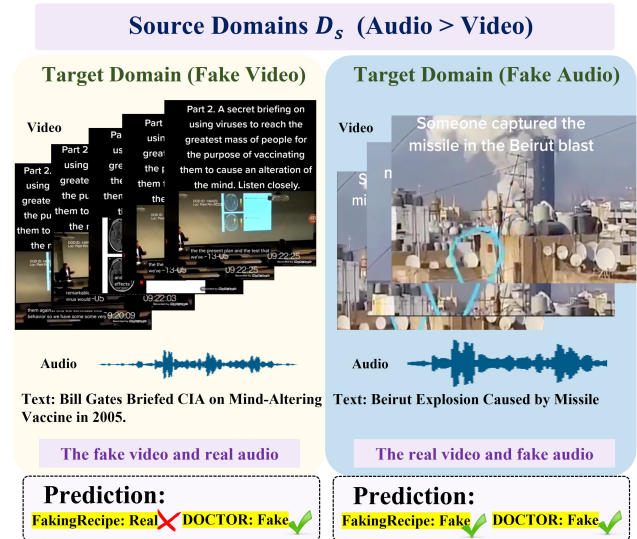


**Figure 4: Case Study illustrating the effectiveness of DOCTOR model in cross-modal forgery detection.**

**4.2.3 Ablation experiments.** To evaluate the effectiveness of each component in the DOCTOR model, we perform comparative analyses by omitting each component individually. The experimental setups are as follows: (1) w/o Diffusion: The diffusion model module is omitted, and fused features are used directly. (2) w/o SE: Semantic and emotion feature fusion is removed. (3) w/o ST: Temporal and spatial feature fusion is removed. (4) w/o Distillation: The interpolation knowledge distillation module is omitted.

As detailed in Table 3, we present the experimental results of the ablation studies. We could observe that the original DOCTOR outperforms all variants, demonstrating the efficacy of each component. Overall, our findings lead to the following conclusions: (1) The importance of spatiotemporal features is usually higher than that of emotional semantic features, which reflects the uniqueness of the spatiotemporal relationship of video angles. (2) The improvement of the diffusion model is slightly better than that of the interpolation distillation, but the difference is not significant, which reflects the common effectiveness of the two.

**4.2.4 Parameter sensitivity analysis.** We systematically evaluate DOCTOR's performance across the learning rate. The results are summarized in Table 4. From the analysis, we observe that the optimal learning rate for DOCTOR varies depending on the dataset: 5e-5 achieves the best performance on the FakeSV dataset, while 1e-3 yields the highest performance on the FakeTT dataset.

**4.2.5 Case study.** As shown in Figure 4, when the model is trained with a focus on audio forgery detection in the source domain, our case study demonstrates that DOCTOR achieves superior



**Figure 5: T-SNE visualizations display the different modal, cross-modal fusion and DOCTOR model. The contents of Figure are as follows: (a) Single frame of video, (b) Video (all frames), (c) Audio, (d) Video-Audio fusion, (e) DOCTOR model (Ours).**

performance in detecting video forgeries in the target domain. This improvement is largely attributed to the use of cross-modal interpolation distillation, which facilitates effective knowledge transfer across modalities and enhances the model’s generalization ability and robustness in cross-modal forgery detection tasks.

**4.2.6 Visualization results.** Due to the domain bias present in videos from different domains, simple fusion techniques may inadvertently amplify this bias. To address this issue, DOCTOR introduces Cross-modal Invariance Fusion to mitigate the impact of domain bias while preserving domain-invariant features. This approach enhances the model’s domain generalization capability for misinformation detection. Additionally, we utilized t-SNE [34] to visualize the features of different modalities and their fusion. As shown in Figure 5. We can find that DOCTOR can effectively reduce domain bias through *Cross modal Invariance Fusion*.

## 5 CONCLUSION

In this paper, we explore the shortcomings of the domain generalization of short-video misinformation detection, which are mainly

divided into two aspects: **(1) Varying Modal-dependence in Different Domains** and **(2) Domain-bias Enhancement in Cross-modal Fusion**. To bridge these gaps, we propose an innovative DDomain generalization model via Consistency and invariance learning for short-video misinformation detection (named DOCTOR). It incorporates two main modules: **(a) Cross-modal Interpolation Distillation** and **(b) Cross-modal Invariance Fusion**. We validate the domain generalization effectiveness of misinformation detection of DOCTOR through comprehensive comparative experiments. In addition, in-depth analysis, including ablation studies, demonstrates the design rationality of each module in the DOCTOR model.

## ACKNOWLEDGMENT

This work was supported by the National Key R&D Program of China under Grant No. 2022YFC3303600, the Zhejiang Provincial Natural Science Foundation of China under Grant No. LY23F020010, and the National Natural Science Foundation of China under Grant Nos. 62337001.

## REFERENCES

- [1] Josh Achiam, Steven Adler, Sandhini Agarwal, Lama Ahmad, Ilge Akkaya, Florencia Leoni Aleman, Diogo Almeida, Janko Altmenschmidt, Sam Altman, Shyamal Anadkat, et al. 2023. Gpt-4 technical report. *arXiv preprint arXiv:2303.08774* (2023).
- [2] Anmol Agarwal, Pratyush Priyadarshi, Shiven Sinha, Shrey Gupta, Hitkul Jangra, Ponnuram Kumaraguru, and Kiran Garimella. 2024. Television discourse decoded: Comprehensive multimodal analytics at scale. In *Proceedings of the 30th ACM SIGKDD Conference on Knowledge Discovery and Data Mining*. 4752–4763.
- [3] Khudejah Ali, Cong Li, Syed Ali Muqtadir, et al. 2022. The effects of emotions, individual attitudes towards vaccination, and social endorsements on perceived fake news credibility and sharing motivations. *Computers in Human Behavior* 134 (2022), 107307.
- [4] Youngmin Baek, Bado Lee, Dongyoon Han, Sangdoon Yun, and Hwalsuk Lee. 2019. Character region awareness for text detection. In *Proceedings of the IEEE/CVF conference on computer vision and pattern recognition*. 9365–9374.
- [5] Yuyan Bu, Qiang Sheng, Juan Cao, Peng Qi, Danding Wang, and Jintao Li. 2023. Combating online misinformation videos: Characterization, detection, and future directions. In *Proceedings of the 31st ACM International Conference on Multimedia*. 8770–8780.
- [6] Yuyan Bu, Qiang Sheng, Juan Cao, Peng Qi, Danding Wang, and Jintao Li. 2024. Fakingrecipe: Detecting fake news on short video platforms from the perspective of creative process. In *Proceedings of the 32nd ACM International Conference on Multimedia*. 1351–1360.
- [7] Sonia Castelo, Thais Almeida, Anas Elghafari, Aécio Santos, Kien Pham, Eduardo Nakamura, and Juliana Freire. 2019. A topic-agnostic approach for identifying fake news pages. In *Companion proceedings of the 2019 World Wide Web conference*. 975–980.
- [8] Yixuan Chen, Dongsheng Li, Peng Zhang, Jie Sui, Qin Lv, Lu Tun, and Li Shang. 2022. Cross-modal ambiguity learning for multimodal fake news detection. In *Proceedings of the ACM web conference 2022*. 2897–2905.
- [9] Hyewon Choi and Youngjoong Ko. 2021. Using topic modeling and adversarial neural networks for fake news video detection. In *Proceedings of the 30th ACM international conference on information & knowledge management*. 2950–2954.
- [10] Jacob Devlin, Ming-Wei Chang, Kenton Lee, and Kristina Toutanova. 2019. Bert: Pre-training of deep bidirectional transformers for language understanding. In *Proceedings of the 2019 conference of the North American chapter of the association for computational linguistics: human language technologies, volume 1 (long and short papers)*. 4171–4186.
- [11] Hao Dong, Ismail Nejjar, Han Sun, Eleni Chatzi, and Olga Fink. 2023. SimMDG: A simple and effective framework for multi-modal domain generalization. *Advances in Neural Information Processing Systems* 36 (2023), 78674–78695.
- [12] Alexey Dosovitskiy, Lucas Beyer, Alexander Kolesnikov, Dirk Weissenborn, Xiaohua Zhai, Thomas Unterthiner, Mostafa Dehghani, Matthias Minderer, G Heigold, S Gelly, et al. 2020. An Image is Worth 16x16 Words: Transformers for Image Recognition at Scale. In *International Conference on Learning Representations*.
- [13] Yunfeng Fan, Wenchao Xu, Haozhao Wang, and Song Guo. 2024. Cross-modal representation flattening for multi-modal domain generalization. *Advances in Neural Information Processing Systems* 37 (2024), 66773–66795.

- [14] Rui Hou, Verónica Pérez-Rosas, Stacy Loeb, and Rada Mihalcea. 2019. Towards automatic detection of misinformation in online medical videos. In *2019 International conference on multimodal interaction*. 235–243.
- [15] Wei-Ning Hsu, Benjamin Bolte, Yao-Hung Hubert Tsai, Kushal Lakhotia, Ruslan Salakhutdinov, and Abdelrahman Mohamed. 2021. Hubert: Self-supervised speech representation learning by masked prediction of hidden units. *IEEE/ACM transactions on audio, speech, and language processing* 29 (2021), 3451–3460.
- [16] Xihang Hu, Fuming Sun, Jing Sun, Fasheng Wang, and Haojie Li. 2024. Cross-modal fusion and progressive decoding network for RGB-D salient object detection. *International Journal of Computer Vision* 132, 8 (2024), 3067–3085.
- [17] Weina Jin, Xiaoxiao Li, and Ghassan Hamarneh. 2022. Evaluating explainable AI on a multi-modal medical imaging task: Can existing algorithms fulfill clinical requirements?. In *Proceedings of the AAAI Conference on Artificial Intelligence*, Vol. 36. 11945–11953.
- [18] Alexander Kirillov, Eric Mintun, Nikhila Ravi, Hanzi Mao, Chloe Rolland, Laura Gustafson, Tete Xiao, Spencer Whitehead, Alexander C Berg, Wan-Yen Lo, et al. 2023. Segment anything. In *Proceedings of the IEEE/CVF international conference on computer vision*. 4015–4026.
- [19] Peiguang Li, Xian Sun, Hongfeng Yu, Yu Tian, Fanglong Yao, and Guangluan Xu. 2021. Entity-oriented multi-modal alignment and fusion network for fake news detection. *IEEE Transactions on Multimedia* 24 (2021), 3455–3468.
- [20] Ruiqi Liu, Boyu Diao, Libo Huang, Zijia An, Zhulin An, and Yongjun Xu. 2024. Continual learning in the frequency domain. *Advances in Neural Information Processing Systems* 37 (2024), 85389–85411.
- [21] Xuannan Liu, Peipei Li, Huaibo Huang, Zekun Li, Xing Cui, Jiahao Liang, Lixiong Qin, Weihong Deng, and Zhaofeng He. 2024. Fka-owl: Advancing multimodal fake news detection through knowledge-augmented lvmis. In *Proceedings of the 32nd ACM International Conference on Multimedia*. 10154–10163.
- [22] Xinran Ma, Mouxiang Yang, Yunfan Li, Peng Hu, Jiancheng Lv, and Xi Peng. 2024. Cross-modal retrieval with noisy correspondence via consistency refining and mining. *IEEE transactions on image processing* (2024).
- [23] Qiong Nan, Juan Cao, Yongchun Zhu, Yanyan Wang, and Jintao Li. 2021. MD-FEND: Multi-domain fake news detection. In *Proceedings of the 30th ACM international conference on information & knowledge management*. 3343–3347.
- [24] Changdae Oh, Junhyuk So, Hoyoon Byun, Yongtaek Lim, Minchul Shin, Jong-June Jeon, and Kyungwoo Song. 2023. Geodesic multi-modal mixup for robust fine-tuning. *Advances in Neural Information Processing Systems* 36 (2023), 52326–52341.
- [25] Yassine Ouali, Adrian Bulat, Brais Matinez, and Georgios Tzimiropoulos. 2023. Black box few-shot adaptation for vision-language models. In *Proceedings of the IEEE/CVF International Conference on Computer Vision*. 15534–15546.
- [26] Hua Pang, Jun Liu, and Jiahui Lu. 2022. Tackling fake news in socially mediated public spheres: A comparison of Weibo and WeChat. *Technology in Society* 70 (2022), 102004.
- [27] Mirco Planamente, Chiara Plizzari, Emanuele Alberti, and Barbara Caputo. 2022. Domain generalization through audio-visual relative norm alignment in first person action recognition. In *Proceedings of the IEEE/CVF winter conference on applications of computer vision*. 1807–1818.
- [28] Peng Qi, Yuyan Bu, Juan Cao, Wei Ji, Ruihao Shui, Junbin Xiao, Danding Wang, and Tat-Seng Chua. 2023. Fakesv: A multimodal benchmark with rich social context for fake news detection on short video platforms. In *Proceedings of the AAAI Conference on Artificial Intelligence*, Vol. 37. 14444–14452.
- [29] Peng Qi, Juan Cao, Xirong Li, Huan Liu, Qiang Sheng, Xiaoyue Mi, Qin He, Yongbiao Lv, Chenyang Guo, and Yingchao Yu. 2021. Improving fake news detection by using an entity-enhanced framework to fuse diverse multimodal clues. In *Proceedings of the 29th ACM International Conference on Multimedia*. 1212–1220.
- [30] Juan Carlos Medina Serrano, Orestis Papakyriakopoulos, and Simon Hegelich. 2020. NLP-based feature extraction for the detection of COVID-19 misinformation videos on YouTube. In *Proceedings of the 1st Workshop on NLP for COVID-19 at ACL 2020*.
- [31] Lanyu Shang, Ziyi Kou, Yang Zhang, and Dong Wang. 2021. A multimodal misinformation detector for covid-19 short videos on tiktok. In *2021 IEEE international conference on big data (big data)*. IEEE, 899–908.
- [32] Amila Silva, Ling Luo, Shanika Karunasekera, and Christopher Leckie. 2021. Embracing domain differences in fake news: Cross-domain fake news detection using multi-modal data. In *Proceedings of the AAAI conference on artificial intelligence*, Vol. 35. 557–565.
- [33] Yu Tong, Weihai Lu, Zhe Zhao, Song Lai, and Tong Shi. 2024. MDMFND: Multi-modal Multi-Domain Fake News Detection. In *Proceedings of the 32nd ACM International Conference on Multimedia*. 1178–1186.
- [34] Laurens Van der Maaten and Geoffrey Hinton. 2008. Visualizing data using t-SNE. *Journal of machine learning research* 9, 11 (2008).
- [35] Longzheng Wang, Chuang Zhang, Hongbo Xu, Yongxiu Xu, Xiaohan Xu, and Siqi Wang. 2023. Cross-modal contrastive learning for multimodal fake news detection. In *Proceedings of the 31st ACM international conference on multimedia*. 5696–5704.
- [36] Tianshi Wang, Fengling Li, Lei Zhu, Jingjing Li, Zheng Zhang, and Heng Tao Shen. 2025. Cross-modal retrieval: a systematic review of methods and future directions. *Proc. IEEE* (2025).
- [37] Zixin Wang, Yadan Luo, Liang Zheng, Zhuoxiao Chen, Sen Wang, and Zi Huang. 2024. In search of lost online test-time adaptation: A survey. *International Journal of Computer Vision* (2024), 1–34.
- [38] Yang Wu, Pengwei Zhan, Yunjian Zhang, Liming Wang, and Zhen Xu. 2021. Multimodal fusion with co-attention networks for fake news detection. In *Findings of the association for computational linguistics: ACL-IJCNLP 2021*. 2560–2569.
- [39] Danni Xu, Shaojing Fan, and Mohan Kankanhalli. 2023. Combating misinformation in the era of generative AI models. In *Proceedings of the 31st ACM International Conference on Multimedia*. 9291–9298.
- [40] Eric Zhongcong Xu, Zeyang Song, Satoshi Tsutsui, Chao Feng, Mang Ye, and Mike Zheng Shou. 2022. Ava-avd: Audio-visual speaker diarization in the wild. In *Proceedings of the 30th ACM International Conference on Multimedia*. 3838–3847.
- [41] An Yang, Baosong Yang, Beichen Zhang, Binyuan Hui, Bo Zheng, Bowen Yu, Chengyuan Li, Dayiheng Liu, Fei Huang, Haoran Wei, et al. 2024. Qwen2. 5 technical report. *arXiv preprint arXiv:2412.15115* (2024).
- [42] Yang Yang, Ran Bao, Weili Guo, De-Chuan Zhan, Yilong Yin, and Jian Yang. 2023. Deep visual-linguistic fusion network considering cross-modal inconsistency for rumor detection. *Science China Information Sciences* 66, 12 (2023), 222102.
- [43] Zhengyuan Yang, Linjie Li, Kevin Lin, Jianfeng Wang, Chung-Ching Lin, Zicheng Liu, and Lijuan Wang. 2023. The dawn of Imms: Preliminary explorations with gpt-4v (ision). *arXiv preprint arXiv:2309.17421* 9, 1 (2023), 1.
- [44] Zhi Zeng, Mingmin Wu, Guodong Li, Xiang Li, Zhongqiang Huang, and Ying Sha. 2023. Correcting the bias: Mitigating multimodal inconsistency contrastive learning for multimodal fake news detection. In *2023 IEEE International Conference on Multimedia and Expo (ICME)*. IEEE, 2861–2866.
- [45] Litian Zhang, Xiaoming Zhang, Chaozhao Li, Ziyi Zhou, Jiacheng Liu, Feiran Huang, and Xi Zhang. 2024. Mitigating social hazards: Early detection of fake news via diffusion-guided propagation path generation. In *Proceedings of the 32nd ACM International Conference on Multimedia*. 2842–2851.
- [46] Litian Zhang, Xiaoming Zhang, Ziyi Zhou, Feiran Huang, and Chaozhao Li. 2024. Reinforced adaptive knowledge learning for multimodal fake news detection. In *Proceedings of the AAAI conference on artificial intelligence*, Vol. 38. 16777–16785.
- [47] Litian Zhang, Xiaoming Zhang, Ziyi Zhou, Xi Zhang, Senzhang Wang, Philip S Yu, and Chaozhao Li. 2024. Early detection of multimodal fake news via reinforced propagation path generation. *IEEE Transactions on Knowledge and Data Engineering* (2024).
- [48] Qiang Zhang, Jiawei Liu, Fanrui Zhang, Jingyi Xie, and Zheng-Jun Zha. 2023. Hierarchical semantic enhancement network for multimodal fake news detection. In *Proceedings of the 31st ACM International Conference on Multimedia*. 3424–3433.
- [49] Wanqing Zhao, Yuta Nakashima, Haiyuan Chen, and Noboru Babaguchi. 2023. Enhancing Fake News Detection in Social Media via Label Propagation on Cross-modal Tweet Graph. In *Proceedings of the 31st ACM International Conference on Multimedia*. 2400–2408.
- [50] Yongchun Zhu, Qiang Sheng, Juan Cao, Qiong Nan, Kai Shu, Minghui Wu, Jindong Wang, and Fuzhen Zhuang. 2022. Memory-guided multi-view multi-domain fake news detection. *IEEE Transactions on Knowledge and Data Engineering* 35, 7 (2022), 7178–7191.
- [51] Ye Zhu, Yu Wu, Nicu Sebe, and Yan Yan. 2024. Vision+ x: A survey on multimodal learning in the light of data. *IEEE Transactions on Pattern Analysis and Machine Intelligence* (2024).
- [52] Linlin Zong, Jiahui Zhou, Wenmin Lin, Xinyue Liu, Xianchao Zhang, and Bo Xu. 2024. Unveiling opinion evolution via prompting and diffusion for short video fake news detection. In *Findings of the Association for Computational Linguistics ACL 2024*. 10817–10826.

## A SPATIAL FEATURE EXTRACTION

We initially utilize a CRAFT OCR [4] to outline the text area ( $TA$ ) of the frame  $F_d$ . Then we adopt the prompt encoder heuristic in the Segment Anything Model (SAM) [18] to convert  $TA$  into prompt embeddings  $X_{vt}^d$  to obtain the feature vector of the location and content information of the text area. At the same time, we input  $F_d$  into the pre-trained ViT to generate the initial encoding  $X_v^d$  to capture the spatial features of the image in a single frame.

For the obtained  $X_{vt}^d$  and  $X_v^d$ , we optimize the representation of visual features  $X_v^d$  through a bidirectional attention mechanism, making it more focused on the relative representation of subtitle features in space. The process mainly takes the following steps:

We input  $X_{vt}^d$  and  $X_v^d$  into a bidirectional attention block. The bidirectional attention block first performs a self-attention (Self-Att) operation on  $X_{vt}^d$  to enhance its own feature representation.

$$\hat{X}_{vt}^d = \frac{(X_{vt}^d + \text{Self-Att}(X_{vt}^d)) - \mu}{\sqrt{\sigma^2 + \epsilon}} \sim \text{NORM}(X_{vt}^d + \text{Self-Att}(X_{vt}^d)) \quad (16)$$

where Self-Att is self-attention, and we normalize all features within the sample to have zero mean and unit variance to help alleviate the problem of internal covariate shift. Later, we use **NORM** to simplify this normalization process. Then, we perform cross-attention (Cross-Att) operations on the optimized features  $\hat{X}_{vt}^d$  and  $X_v^d$  to interact with each other and further optimize the  $\hat{X}_{vt}^d$ .

$$\hat{X}_{vt}^d = \text{NORM}(\hat{X}_{vt}^d + \text{Cross-Att}(\hat{X}_{vt}^d, X_v^d)) \quad (17)$$

Lastly, a cross-attention operation is performed on  $X_v^d$  to make it interact with the updated  $\hat{X}_{vt}^d$  from MLP to obtain a more accurate visual feature representation.

$$\hat{X}_v^d = \text{NORM}(X_v^d + \text{Cross-Att}(\text{MLP}(\hat{X}_{vt}^d), X_v^d)) \quad (18)$$

After the attention process, the updated  $\hat{X}_v^d$  is down-sampled through two convolutional layers and then expanded to obtain the spatial pattern features of a single frame  $X^d$ . Finally, we use self-attention to fuse these single-frame spatial features and obtain a unified spatial feature representation through average pooling (MEAN).

$$X_{spa} = \text{MEAN}(\text{Self-Att}([X^1, X^2, \dots, X^d])) \quad (19)$$

## B DOMAIN DATASETS

**Table 5: Domains division of FakeSV and FakeTT datasets.**

Domain	FakeSV	FakeTT
Culture	278	325
Disaster	1836	182
Education	195	28
Finance	116	9
Health	841	121
Politics	296	715
Military	121	84
Science	234	271
Society	1621	337

We use the Qwen2.5-72B [41] combined with manual verification for label classification based on the text and fakesv’s video collection introduction [28]. We divide the above two datasets into nine domains, respectively. Specific domains’ names and numbers are detailed and shown in Table 5.

The specific prompt template is: “Here are some fields: Society, Health, Disaster, Culture, Education, Finance, Politics, Science, Military. And some examples from different domains [Some examples (Society: [case text], Health: [case text], ...)]. You can then compare and analyze the [input text] with the examples above to choose the most suitable Domain.”

We divide the above two datasets into nine domains, respectively. Specific domains’ names and numbers are detailed and shown in Table 5. Since the number of some domains is small (Education, Finance, and Military in the FakeTT dataset), we conduct merging experiments with them.

## C MORE EXPERIMENTAL ANALYSES

### C.1 Training Strategy

We define the total loss function  $Loss_{\text{final}}$  as the combination of the **Cross-modal Interpolation Distillation** loss  $Loss_{\text{dis}}$  and the **Cross-modal Invariance Fusion** loss  $Loss_{\text{es}}$  (emotion and sentiment features) and  $Loss_{\text{st}}$  (spatial and temporal features). The specifically  $Loss_{\text{final}}$  we define is as follows:

$$Loss_{\text{final}} = \alpha Loss_{\text{es}} + \beta Loss_{\text{st}} + \gamma Loss_{\text{dis}}, \quad (20)$$

where  $\alpha$ ,  $\beta$ , and  $\gamma$  denote the weighting factors.

### C.2 Experimental Implementations

Our experiments include two aspects: domain generalization experiments and general domain experiments. The comparison methods selected in the domain generalization experiments are mainly the best performing and latest methods selected from general domain experiments for comparison. All our experiments were conducted on an NVIDIA RTX A6000 (48G). The  $\alpha$  in the loss functions  $Loss_{\text{final}}$  is 0.1,  $\beta$  is 3, and  $\gamma$  is 0.05. We choose the learning rates of 5e-5 for FakeSV and 1e-3 for FakeTT.

For more details on the DOCTOR model, our anonymous source code is available at <https://anonymous.4open.science/r/DOCTOR-D1D2>.

### C.3 Comparison of Domain Generalization Star Map

As shown in Figure 6, the experiment present a comparative analysis of six misinformation detection methods (FakingRecipe, SV-FEND, OpEvFake, CMRF\*, MMDFND\*, and DOCTOR) across two distinct datasets: FakeSV and FakeTT. The radar visualization effectively illustrates each method’s performance across multiple content categories, including Disaster, Society, Health, Culture, Politics, Science, Education, Finance, and Military for FakeSV, with a combined Education/Finance/Military category for FakeTT. The charts reveal DOCTOR consistently outperforming other methods across most categories in both datasets, particularly excelling in Military (93.65%) for FakeSV and Culture (88.31%) for FakeTT.

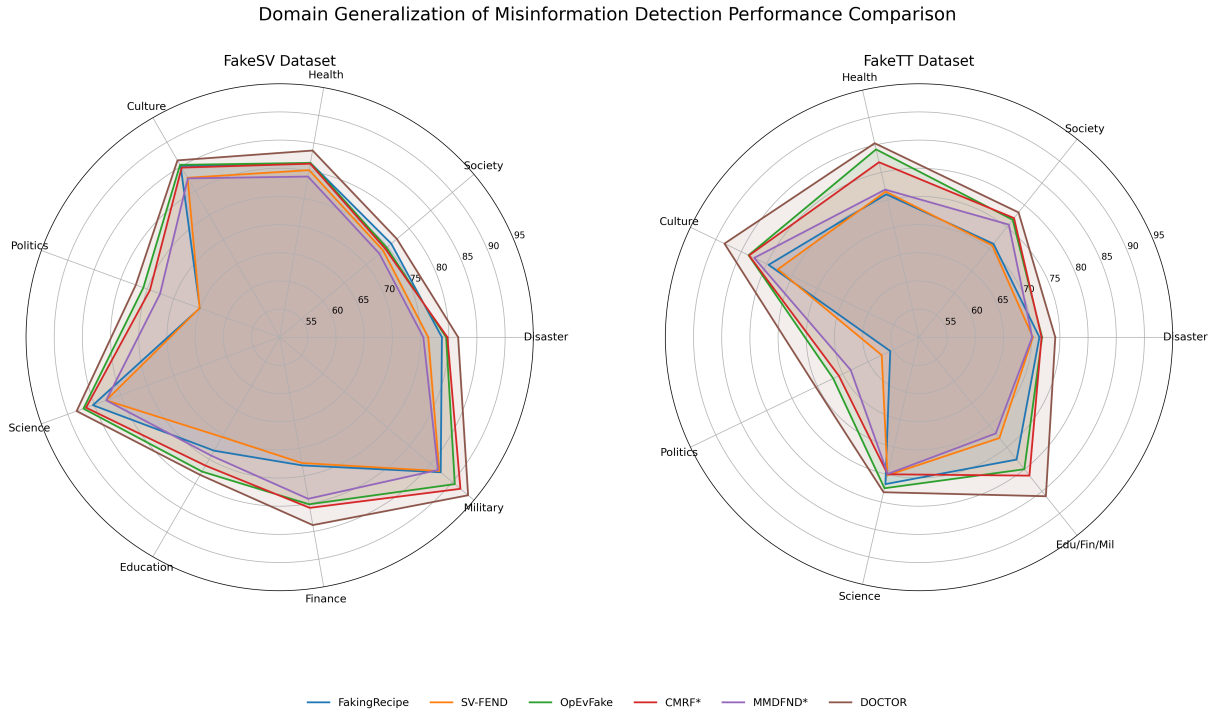


**Figure 6: Comparative analysis of six misinformation detection methods (FakingRecipe, SV-FEND, OpEvFake, CMRF\*, MMDFND\*, and DOCTOR) across two distinct datasets: FakeSV and FakeTT. \* represents the domain generalization method.**

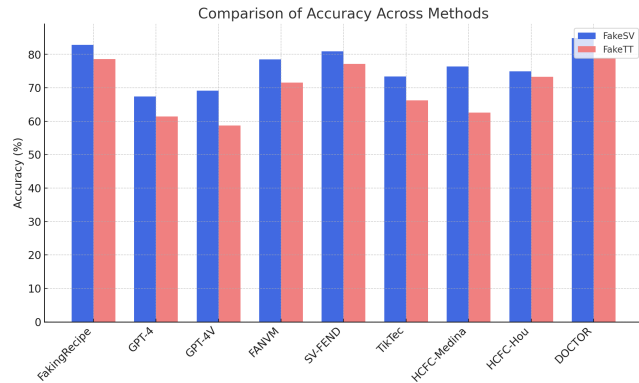


**Figure 7: Accuracy comparison of different methods on FakeSV and FakeTT datasets.**

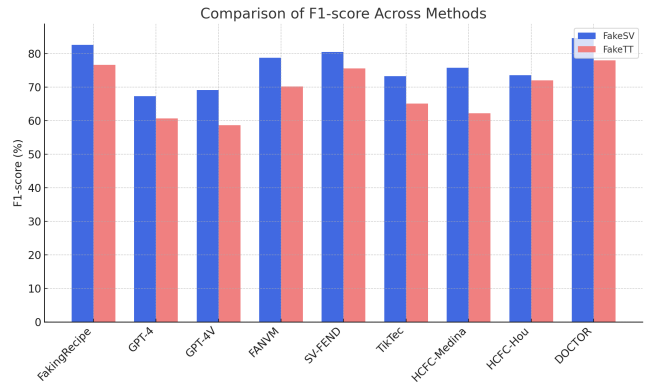


**Figure 8: F1 comparison of different methods on FakeSV and FakeTT datasets.**

### C.4 More comparative accuracy analysis

The above two figures of Figure 7 and Figure 8 show the comparison of the Accuracy and F1-score of different methods on FakeSV and FakeTT datasets. It can be seen that the DOCTOR method achieved the best performance on both datasets.

The above three figures of Figure 11, Figure 10, and Figure 9 show the comparison of the Precision, Recall, and F1-score of different methods on the Fake category on the FakeSV and FakeTT datasets. It can be seen that the DOCTOR method performs outstandingly in Recall and F1-score on the Fake category.

The above three figures of Figure 14, Figure 13, and Figure 12 show the comparison of the Precision, Recall, and F1-score of the Real category of different methods on the FakeSV and FakeTT datasets. From the results, the DOCTOR method performs best in Precision while maintaining a high level in Recall and F1-score, and the overall performance is stable.

### C.5 Discussion on DOCTOR Model Efficiency

Despite the advanced features and complex mechanisms integrated into the DOCTOR model, as shown in Figure 15, our experiments

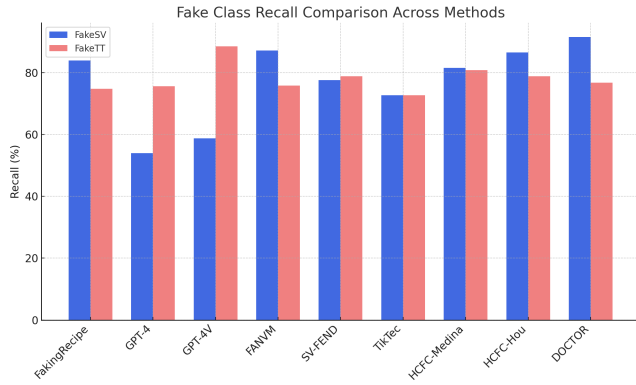


**Figure 9: Recall comparison of different methods on FakeSV and FakeTT datasets (Fake class).**

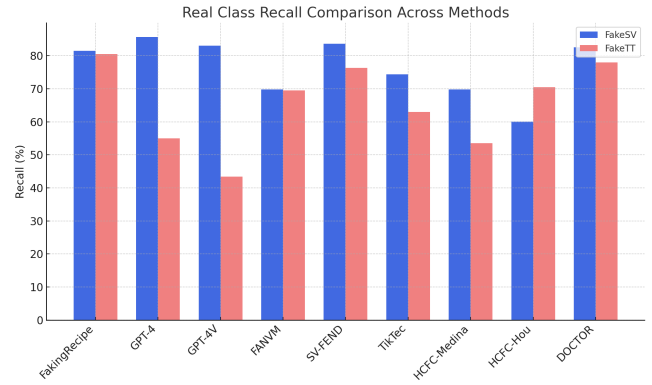


**Figure 12: Recall comparison of different methods on FakeSV and FakeTT datasets (Real class).**

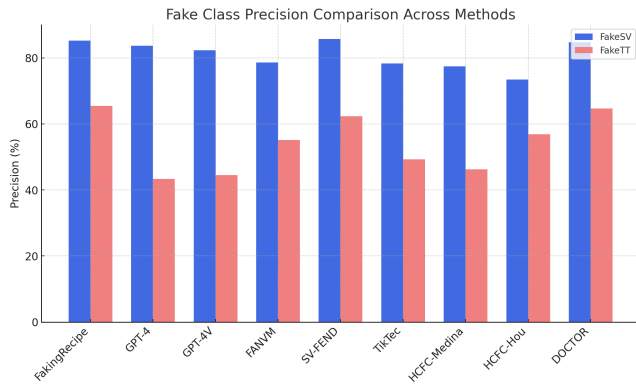


**Figure 10: Precision comparison of different methods on FakeSV and FakeTT datasets (Fake class).**

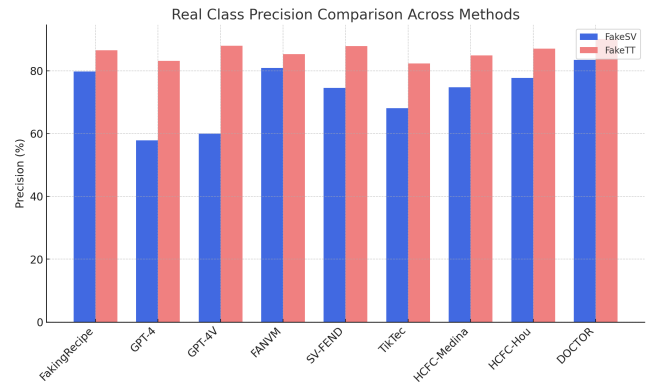


**Figure 13: Precision comparison of different methods on FakeSV and FakeTT datasets (Real class).**

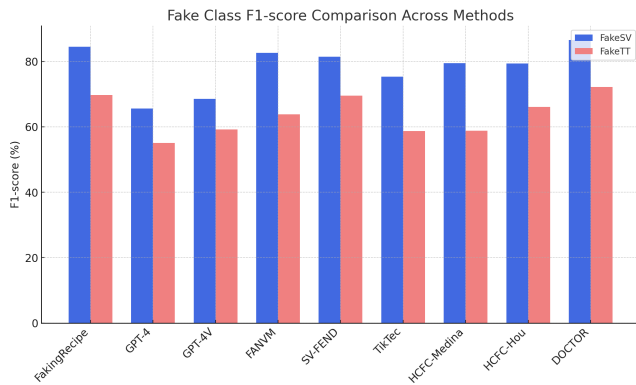


**Figure 11: F1 comparison of different methods on FakeSV and FakeTT datasets (Fake class).**

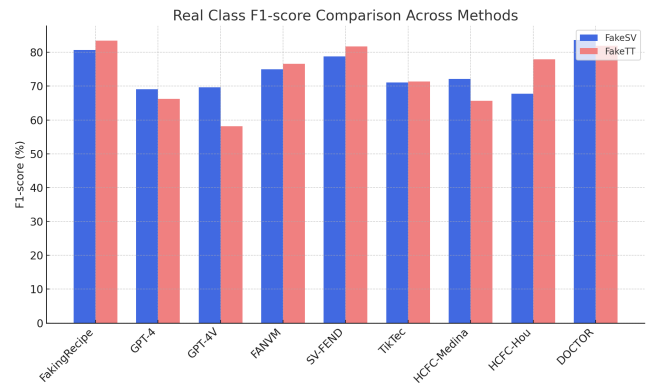


**Figure 14: F1 comparison of different methods on FakeSV and FakeTT datasets (Real class).**

reveal that the computational overhead does not experience a significant increase. The incorporation of cross-modal interpolation distillation and multi-modal invariance fusion, while enhancing the model’s generalization ability across different domains, does not lead

to a substantial rise in computational cost. This indicates that DOCTOR is able to maintain efficient performance, even with the addition of multiple modalities and the complexity of noise-based feature refinement. The efficiency of DOCTOR is crucial for real-world

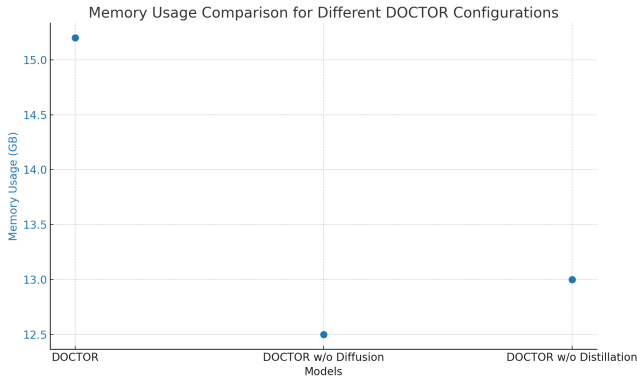


Figure 15: Discussion on DOCTOR Model Efficiency.

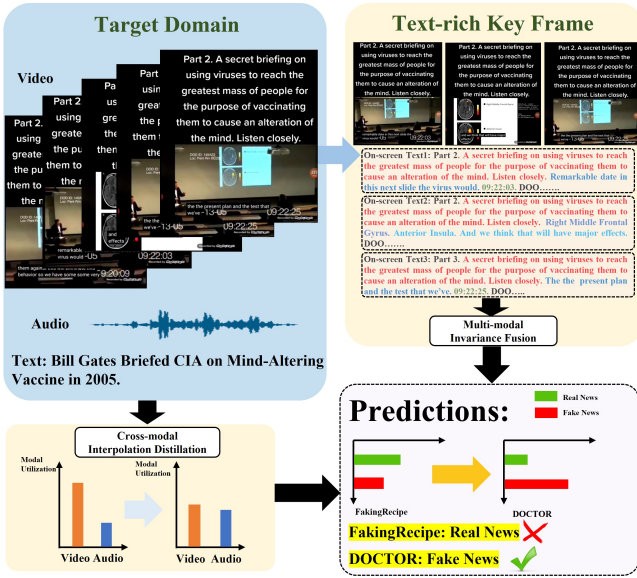


Figure 16: Case: Bill Gates Briefed CIA on Mind-Altering Vaccine in 2005.

applications, where both accuracy and computational efficiency are paramount.

### C.6 Case Study

As shown in Figure 16. Case: Bill Gates Briefed CIA on Mind-Altering Vaccine in 2005.

In this case, the DOCTOR model demonstrates strong domain generalization capabilities by correctly identifying the video as misinformation, while traditional methods like FakingRecipe misclassify it as truth. They struggle to adapt when encountering unseen distributions, variations in video styles, or novel linguistic manipulations. In contrast, DOCTOR incorporates multi-modal invariance fusion and cross-modal interpolation distillation, allowing it to generalize across different domains by capturing latent relationships between text, audio, and video. This enables it to detect cross-modal

inconsistencies, making it more robust against out-of-domain misinformation scenarios.

## D TEMPORAL POSITION ENCODING

**Temporal Position Encoding (TPE)** is designed to capture the coarse temporal location of each segment within the entire video. To achieve this, we divide the video into  $B$  equal-frequency temporal bins and assign each segment to one of them based on its position in the sequence. Each bin is associated with a learnable embedding vector, which is used to represent the temporal context of segments assigned to that bin. This encoding helps the model understand whether a segment is located at the beginning, middle, or end of the video, which can be crucial for modeling temporal editing patterns.

### Algorithm 2 Temporal Position Encoding (TPE)

**Require:** Number of segments  $n$ , number of bins  $B$ , embedding dimension  $d$

**Ensure:** Temporal position embeddings  $\{TPE^1, \dots, TPE^n\}$

- 1:  $s \leftarrow \lfloor \frac{n}{B} \rfloor$
- 2: Initialize embedding matrix  $E \in \mathbb{R}^{B \times d}$
- 3: **for**  $i = 1$  **to**  $n$  **do**
- 4:  $b_i \leftarrow \min\left(\lfloor \frac{i-1}{s} \rfloor, B-1\right)$
- 5:  $TPE^i \leftarrow E[b_i]$
- 6: **end for**
- 7: **return**  $\{TPE^1, \dots, TPE^n\}$

## E DURATION ENCODING

**Duration Encoding (DE)** encodes the fine-grained temporal position of each segment using a fixed sinusoidal scheme, similar to the original positional encoding used in Transformers. This method ensures that each segment has a unique continuous representation based on its position index. For each segment  $i$ , and for each embedding dimension  $j$ , the encoding alternates between sine and cosine functions of different frequencies. This encoding provides precise temporal cues, enabling the model to capture temporal dependencies and alignment across modalities.

### Algorithm 3 Duration Encoding (DE)

**Require:** Number of segments  $n$ , encoding dimension  $d$

**Ensure:** Duration encodings  $\{DE^1, \dots, DE^n\}$

- 1: Initialize  $DE \in \mathbb{R}^{n \times d}$  with zeros
- 2: **for**  $i = 0$  **to**  $n-1$  **do**
- 3: **for**  $j = 0$  **to**  $d-1$  **do**
- 4:  $\theta \leftarrow \frac{i}{10000 \cdot \frac{2 \cdot \lfloor j/2 \rfloor}{d}}$
- 5: **if**  $j$  is even **then**
- 6:  $DE^{i+1}[j] \leftarrow \sin(\theta)$
- 7: **else**
- 8:  $DE^{i+1}[j] \leftarrow \cos(\theta)$
- 9: **end if**
- 10: **end for**
- 11: **end for**
- 12: **return**  $\{DE^1, \dots, DE^n\}$

## F PREDICATION

---

### Algorithm 4 Prediction via Feature Diffusion and Distillation Fusion

---

```

1: Input: Time feature  $X_{\text{time}}$ , Spatial feature  $X_{\text{spa}}$ ,
   Semantic feature  $X_{\text{sem}}$ , Emotional feature  $X_{\text{emo}}$ ,
   Video feature  $X_{\text{video}}$ , Audio feature  $X_{\text{audio}}$ 
2: Output: Final prediction score  $\hat{Y}_{\text{final}}$ 
3: {Step 1: Feature fusion and diffusion}
4:  $X_{\text{all}} \leftarrow \text{Concatenate}(X_{\text{time}}, X_{\text{spa}}, X_{\text{sem}}, X_{\text{emo}})$ 
5:  $X_{\text{diffused}} \leftarrow \text{ApplyDiffusion}(X_{\text{all}})$ 
6: {Step 2: Time and space prediction branch}
7:  $X_{\text{ts}} \leftarrow \text{Extract}(X_{\text{diffused}}, [\text{time}, \text{spa}])$ 
8:  $\hat{Y}_{\text{st}} \leftarrow \text{MLP}_{\text{TS}}(X_{\text{ts}})$ 
9: {Step 3: Semantic and emotional prediction branch}
10:  $X_{\text{se}} \leftarrow \text{Extract}(X_{\text{diffused}}, [\text{sem}, \text{emo}])$ 
11:  $\hat{Y}_{\text{es}} \leftarrow \text{MLP}_{\text{SE}}(X_{\text{se}})$ 
12: {Step 4: Video-Audio distillation output}
13:  $\hat{Y}_{\text{dis}} \leftarrow \text{Distill}(X_{\text{video}}, X_{\text{audio}})$ 
14: {Step 5: Late fusion to get final prediction}
15:  $\hat{Y}_{\text{fusion}} \leftarrow \hat{Y}_{\text{st}} \times \tanh(\hat{Y}_{\text{es}})$ 
16:  $\hat{Y}_{\text{final}} \leftarrow \hat{Y}_{\text{fusion}} \times \hat{Y}_{\text{dis}}$ 
17: return  $\hat{Y}_{\text{final}}$ 

```

---

To generate the final prediction, we design a multi-branch architecture that integrates temporal, spatial, semantic, and emotional features through a diffusion-enhanced fusion mechanism. As illustrated in Algorithm 4, the input features  $X_{\text{time}}$ ,  $X_{\text{spa}}$ ,  $X_{\text{sem}}$ , and  $X_{\text{emo}}$  are first concatenated and passed through a diffusion process to enhance inter-feature dependencies and latent structure alignment. The diffused representation  $X_{\text{diffused}}$  is then split into two branches:

**Time-Spatial Branch:** We extract the time and spatial-related features to form  $X_{\text{ts}}$ , which is passed through a dedicated  $\text{MLP}_{\text{TS}}$  to yield an intermediate prediction  $\hat{Y}_{\text{st}}$ .

**Semantic-Emotional Branch:** Similarly, semantic and emotional components are extracted as  $X_{\text{se}}$ , which is processed via another  $\text{MLP}_{\text{SE}}$  to produce  $\hat{Y}_{\text{es}}$ .

In parallel, we distill information from both video and audio modalities using a specialized distillation module, resulting in  $\hat{Y}_{\text{dis}}$ .

For final prediction, we adopt a late fusion strategy where the time-spatial output is modulated by the nonlinear activation of the semantic-emotional output:  $\hat{Y}_{\text{fusion}} = \hat{Y}_{\text{st}} \cdot \tanh(\hat{Y}_{\text{es}})$ . This fusion is then further modulated by the distilled multi-modal prediction:  $\hat{Y}_{\text{final}} = \hat{Y}_{\text{fusion}} \cdot \hat{Y}_{\text{dis}}$ . This design effectively captures complementary information from all feature domains and ensures robustness through multi-modal consistency.

For specific code implementation, please refer to the code link.